MOBILE ROBOT OBSTACLE DETECTION USING AN OVERLAPPED ULTRASONIC SENSOR RING

Sungbok Kim, Jaehee Jang and Hyun Bin Kim
Department of Digital Information Engineering, Hankuk University of Foreign Students, Korea

Keywords: Ultrasonic Sensor, Overlapped Beam Pattern, Positional Uncertainty, Obstacle Position, Sensor Model.

Abstract: This paper presents the obstacle detection of a mobile robot using an ultrasonic sensor ring with overlapped beam pattern. Basically, it is assumed that a set of ultrasonic sensors are installed at regular intervals along the side of a circular mobile robot of nonzero radius. First, by exploiting the overlapped beam pattern, it is shown that the positional uncertainty inherent to an ultrasonic sensor can be significantly reduced for both single and double obstacle detection. Second, given measured distances from adjacent ultrasonic sensors, the geometric method of computing the position of the detected obstacle with respect to the center of a mobile robot is described. Third, through experiments using our ultrasonic sensor ring prototype, the validity and the performance of the proposed overlapped ultrasonic sensor ring are demonstrated.

1 INTRODUCTION

Since the mid 1980s, ultrasonic sensors have been widely used for map building and obstacle avoidance. Typically, an ultrasonic sensor equipped at a mobile robot operates in reflective mode, rather than in direct wave mode. Once the acoustic wave is emitted by the transmitter, an ultrasonic sensor can measure the obstacle distance using the elapsed time until the reflected wave is sensed by the receiver, which is called the time of flight. The detected obstacle is present at a certain point along the arc of radius given by the obstacle distance; however, the exact position of an obstacle on the arc remains unknown. This is called the positional uncertainty inherent to an ultrasonic sensor.

To alleviate the problem of positional uncertainty, we propose to overlap the cone shaped beams of two ultrasonic sensors in part. With the overlapped beam pattern, the entire sensing zone of each ultrasonic sensor can be divided into two smaller sensing subzones: the overlapped and the unoverlapped subzones. If both ultrasonic sensors detect an obstacle, the detected obstacle should belong to the overlapped subzone. On the other hand, if either ultrasonic sensor detects an obstacle, the detected obstacle should belong to the unoverlapped subzone. This indicates that the positional uncertainty of an ultrasonic sensor can be reduced by exploiting the overlapped beam pattern of two ultrasonic sensors. In this paper, we present the obstacle detection of a mobile robot using an ultrasonic sensor ring with overlapped beam pattern.

2 POSITIONAL UNCERTAINTY REDUCTION

Assume that N ultrasonic sensors of the same type are arranged in a circle at regular intervals with their beams overlapped. After numbering the ultrasonic sensors from 1 to N in clockwise order, let S_k, $k = 1, \cdots, N$, denote the k^{th} ultrasonic sensor of an overlapped ultrasonic sensor ring. Fig. 1 shows three adjacent ultrasonic sensors, S_N, S_1, and S_2, which are placed at the left, the center, and the right, respectively. Due to beam overlapping, the entire sensing zone of the ultrasonic sensor S_1 can be divided into three sensing subzones, denoted by 'I', 'II', and 'III'. In Fig.1, an obstacle P is depicted by a bold.

First, let us consider the detection of a single obstacle using three overlapped ultrasonic sensors. Let ρ_N, ρ_1, and ρ_2 be the distances of the obstacle P measured by three ultrasonic sensors, S_N, S_1, and S_2, respectively. Table 1 shows the distance measurements of S_N, S_1, and S_2, depending on to the position of P among one of three sensing

Kim S., Jang J. and Kim H. (2010).
MOBILE ROBOT OBSTACLE DETECTION USING AN OVERLAPPED ULTRASONIC SENSOR RING.
In *Proceedings of the 7th International Conference on Informatics in Control, Automation and Robotics*, pages 340-343
DOI: 10.5220/0002878803400343

subzones, either I, II, or III. In Table 1, '∞' indicates the situation that P cannot be detected by the corresponding ultrasonic sensor. Seen from Table 1, the combination of three ultrasonic sensors which return finite measured distances varies according to where the obstacle belongs among three sensing subzones. This implies that the sensing subzone to which the obstacle belongs can be determined based on the combination of three ultrasonic sensors returning finite measured distances. It should be noted that the beam overlapping between adjacent ultrasonic sensors can lead to the significant reduction in positional uncertainty.

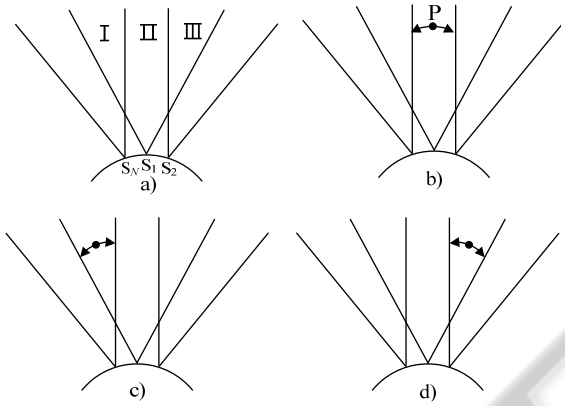

Figure 1: Single obstacle detection using overlapped ultrasonic sensors.

Table 1: Distance measurements of ultrasonic sensors in the case of single obstacle detection.

	2b)	2c)	2d)
P	II	I	III
S_N	∞	ρ_N	∞
S_1	ρ_1	ρ_1	ρ_1
S_2	∞	∞	ρ_2

Next, let us consider the detection of double obstacles using three overlapped ultrasonic sensors. Note that the number of obstacles that can be detected by two adjacent ultrasonic sensors is at most two, regardless of how many obstacles are present in front of them. Assume that one obstacle is present at far distance, called the far obstacle and denoted by P_f, and the other obstacle is present at the near distance, called the near obstacle and denoted by P_n. Fig. 2 shows three different cases of how the far and near obstacles are located. Let $\rho_{f,i}$ and $\rho_{n,i}$ $(< \rho_{f,i})$, $i = N, 1, 2$, be the distances of the obstacles, P_f and P_n, measured by three ultrasonic sensors, S_N, S_1, and S_2, respectively.

Table 2 shows the distance measurements of three ultrasonic sensors, S_N, S_1, and S_2, depending on the relative positions of the far and the near obstacles, P_f and P_n. Referring to Table 2, the following decisions can be made on where P_f and P_n are positioned among three sensing subzones, I, II, and III. For instance, if the left ultrasonic sensor S_N returns larger value than the other two ultrasonic sensors, S_1 and S_2, as shown in Fig. 2a), P_f is positioned within I and P_n is positioned within III.

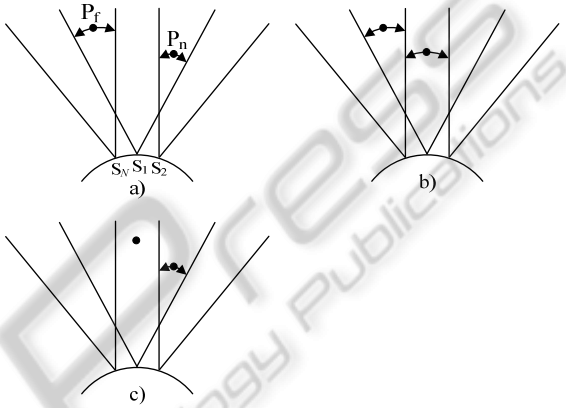

Figure 2: Double obstacle detection using overlapped ultrasonic sensors.

Table 2: Distance measurements of ultrasonic sensors in the case of double obstacle detection.

	3a)	3b)	3c)
P_f	I	I	II
P_n	III	II	III
S_N	$\rho_{f,N}$	$\rho_{f,N}$	∞
S_1	$\rho_{n,1}$	$\rho_{n,1}$	$\rho_{n,1}$
S_2	$\rho_{n,2}$	∞	$\rho_{n,2}$

3 MOBILE ROBOT REFERENCED OBSTACLE DETECTION

Each ultrasonic sensor of an ultrasonic sensor ring returns the distance of an obstacle that is measured with reference to the vertex of its own, called the sensor referenced obstacle distance. On the other hand, it is the obstacle position with reference to the center of a mobile robot, called the mobile robot referenced obstacle position that should be known for the obstacle detection/avoidance of a navigating

mobile robot.

First, suppose that an obstacle P is present at the distance ρ_1 within the unoverlapped sensing subzone II of the ultrasonic sensor S_1, as shown in Fig. 3. Let G_1 and F_1 denote the intersecting points of the circle of radius ρ_1 centered at the point S_1, and the right beam boundary of the ultrasonic sensor S_N and the right beam boundary of the ultrasonic sensor S_2, respectively.

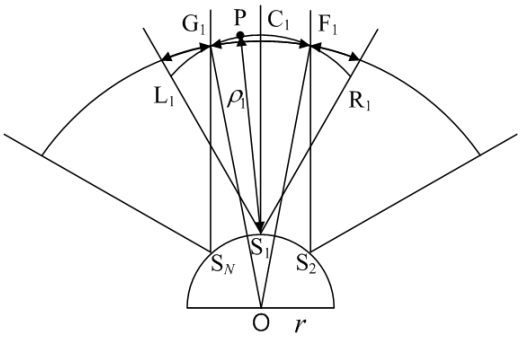

Figure 3: The mobile robot referenced position of an obstacle within the unoverlapped sensing zone.

Due to the positional uncertainty, an obstacle P can exist at a certain point along the arc $\widehat{G_1C_1F_1}$ of radius ρ_1 centered at the point S_1, instead of the arc $\widehat{L_1C_1R_1}$. Considering that the ultimate goal of obstacle detection is to prevent possible collision with obstacles, it is reasonable to take conservative stance in guessing the obstacle position. To prepare for the worst case scenario, the collision free region can be specified as the intersection of the circle of radius $\overline{OF_1}$ centered at the point O and the cone of angle $\angle G_1OF_1$ centered along the line $\overline{OC_1}$. As a result of the beam overlapping of an ultrasonic sensor ring, 1) the radius of the collision free region increases, that is, $\overline{OF_1} > \overline{OR_1}$, and 2) the angle of the collision free region decreases, that is, $\angle G_1OF_1 < \angle L_1OR_1$. The increased radius can allow a mobile robot more room for obstacle avoidance, and the decreased angle can improve the spatial resolution in obstacle detection.

Next, suppose that an obstacle P is present at the distance ρ_1 within the overlapped sensing subzone III of the ultrasonic sensor S_1, as shown in Fig. 7. Let ρ_1 and ρ_2 be the distance of P from the vertices of ultrasonic sensors, S_1 and S_2, respectively. Owing to the positional uncertainty of two ultrasonic sensors, P exists along the arc $\widehat{L_1R_1}$ of radius ρ_1 centered at the point S_1, and it also exists along the arc $\widehat{L_2R_2}$ of radius ρ_2 centered at the point S_2. As shown in Fig. 4, the position of P can now be obtained from the intersection of these two circles, which results in two intersecting points in general. Finally, the obstacle position can be uniquely determined out of two intersecting points, based on the relative locations of ultrasonic sensors, S_1 and S_2. It should be noted that the problem of uncertainty does not exist anymore for an obstacle within the overlapped sensing subzone, although the measurement errors may still affect the accuracy in computing the obstacle position.

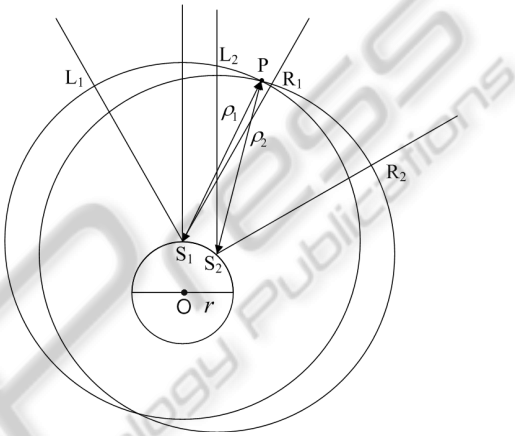

Figure 4: The mobile robot referenced position of an obstacle within the overlapped sensing subzone.

4 EXPERIMENTAL RESULTS

An omnidirectional overlapped ultrasonic sensor ring prototype was built using the ultrasonic sensor modules which contain MA40B8 of beam width $\alpha = 50°$ from Murata Inc. As shown in Fig. 5, twelve ultrasonic sensor modules are first installed at a regular spacing of $\beta = 30°$ between two circular acrylic plates of radius $r = 19\,\text{cm}$, which is then fixed on top of a circular mobile robot concentrically.

First, a mobile robot is commanded to move along a straight line, which is 1 m apart from a circular obstacle of diameter 12.5 cm. Fig. 6 shows the division of the straight line depending on the combination of ultrasonic sensors involved in obstacle detection. It can be observed that the distance from P_1 to P_3 is about 170 cm and the distance from P_2 to P_5 is about 140 cm. Using these data, the effective beam widths can be calculated: 70° for the center ultrasonic sensor and 60° for the left and right ultrasonic sensors.

Figure 5: Our overlapped ultrasonic sensor ring prototype.

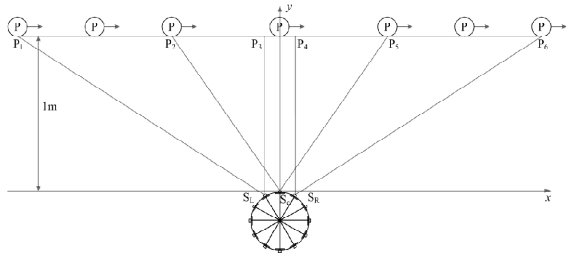

Figure 6: The experimental results for single obstacle detection.

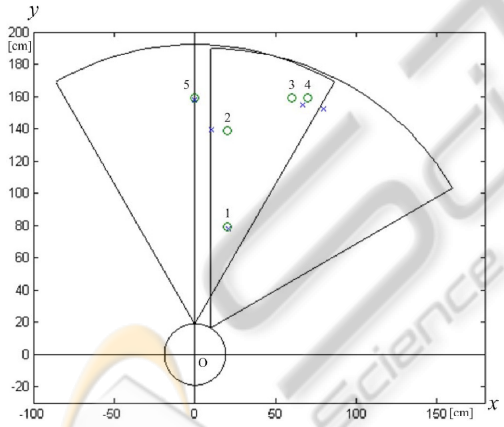

Figure 7: The experimental setting and results for computing mobile robot referenced obstacle positions.

Next, for five different locations of an obstacle, we compute the mobile robot referenced position of an obstacle from the measured distances of three ultrasonic sensors. Fig. 7 shows the actual and the computed obstacle positions, which are marked by 'o' and 'x', respectively. The discrepancy between the actual and the computed obstacle positions tends to increase as an obstacle is located away from the center of the overlapped ultrasonic sensor ring and close to the boundary of the overlapped sensing subzone. However, it is confirmed through repetitive experiments that the maximum discrepancy is bounded within 10 cm.

5 CONCLUSIONS

In this paper, we proposed an overlapped ultrasonic sensor ring which consists of relatively small number of low cost ultrasonic sensors with low directivity, to reduce the positional uncertainty in obstacle detection. The proposed ultrasonic sensor ring made of low directivity ultrasonic sensors is advantageous over its high directivity counterpart in both sensor device and data processing requirements. It is expected that the results of this paper can facilitate early deployment of low cost mobile platforms for personal service robots.

REFERENCES

Borenstein, J. and Koren, J., 1989. Real-Time Obstacle Avoidance for Fast Mobile Robots. In *IEEE Trans. Sysems, Man, and Cybernetics*, vol. 19, no. 5, pp. 1179-1187.

Choset, H., Nagatani, K., and Lazar, N. A., 2003. The Arc-Traversal Median Algorithm: A Geometric Approach to Increase Ultrasonic Sensor Azimuth Accuracy. In *IEEE Trans. Robotics and Automation*, vol. 19, no. 3, pp. 513-522.

Crowley, J. L., 1989. World Modeling and Position Estimation for a Mobile Robot Using Ultrasonic Ranging. In *Proc. IEEE Int. Conf. Robotics and Automation*, pp. 674-680.

Elfes, A., 1987. Sonar-Based Real-World Mapping and Navigation. In *IEEE J. Robotics and Automation*, vol. RA-3, no. 3, pp. 249-265.

McKerrow, P. J., 1993. Echolocation-from Range to Ontline Segments. In *Robotics and Autonomous Systems*, vol. 11, no. 4, pp. 205-211.

Moravec, H., and Elfes, A., 1985. High Resolution Maps for Wide Angles Sonar. In *Proc. IEEE Int. Conf. Robotics and Automation*, pp. 116-121.

Murphy, R., 2000. *Introduction to AI Robotics,* The MIT Press.

Thrun, S., Burgard, W., and Fox, D., 2005. *Probabilistic Robotics,* The MIT Press.

Wijk, O. and Christensen, H. I., 2000. Triangulation-Based Fusion of Sonar Data with Application in Robot Pose Tracking. In *IEEE Trans. Robotics and Automation*, vol. 16, no. 6, pp. 740-752.